DEVELOPMENTAL BIOLOGY

Lacrimal gland budding requires PI3K-dependent suppression of EGF signaling

Qian Wang[1], Chenqi Tao[1†], Abdul Hannan[1†], Sungtae Yoon[1], Xuanyu Min[1], John Peregrin[1], Xiuxia Qu[2], Hongge Li[1‡], Honglian Yu[1,3], Jean Zhao[4], Xin Zhang[1]*

The patterning of epithelial buds is determined by the underlying signaling network. Here, we study the cross-talk between phosphoinositide 3-kinase (PI3K) and Ras signaling during lacrimal gland budding morphogenesis. Our results show that PI3K is activated by both the p85-mediated insulin-like growth factor (IGF) and Ras-mediated fibroblast growth factor (FGF) signaling. On the other hand, PI3K also promotes extracellular signal–regulated kinase (ERK) signaling via a direct interaction with Ras. Both PI3K and ERK are upstream regulators of mammalian target of rapamycin (mTOR), and, together, they prevent expansion of epidermal growth factor (EGF) receptor expression from the lacrimal gland stalk to the bud region. We further show that this suppression of EGF signaling is necessary for induction of lacrimal gland buds. These results reveal that the interplay between PI3K, mitogen-activated protein kinase, and mTOR mediates the cross-talk among FGF, IGF, and EGF signaling in support of lacrimal gland development.

INTRODUCTION

Glandular organs are formed via the process of branching morphogenesis, which in essence is a reiterative cycle of budding and elongation of epithelial tubes (*1*). To produce the stereotypical pattern of branching in each organ, however, the competition between budding and elongation must be tightly controlled in a tissue-specific manner. This balance is shaped by the local mesenchyme that provides the unique environmental cue and by the intrinsic molecular network that determines the identity of the epithelium.

The lacrimal gland secretes the aqueous layer of the tear film, which is crucial for nourishing and protecting the ocular surface (*2*, *3*). During murine embryogenesis, the lacrimal gland arises as a thickening epithelium from the conjunctiva, before invading into the periocular mesenchyme to form an enlarged bud followed by an elongated stalk (Fig. 1A) (*4*). This eventually develops into a bipartite structure of intra- and extraorbital glands (iLG and eLG), each consisting of dense networks of ducts and acini (Fig. 1A). Many extracellular factors have been implicated in lacrimal gland development, the most prominent among which is fibroblast growth factor (FGF) (*4*). Previous studies have established that lacrimal gland development is induced by the mesenchyme-derived Fgf10, which binds Fgfr2b on the conjunctival epithelium in the presence of heparan sulfate proteoglycans (*5*–*7*). FGF-induced Ras/mitogen-activated protein kinase (MAPK) signaling in the epithelium targets the Pea3 family transcription factors to specify the lacrimal gland cell fate (*8*, *9*). On the other hand, Shp2 (Src homology region 2 domain-containing phosphatase-2)–mediated FGF-Ras-MAPK signaling in the neural crest controls expression of homeodomain protein Alx4,

which promotes the periocular mesenchyme to produce Fgf10 (*10*). Thus, Ras-MAPK signaling is essential for the formation of both the epithelial and mesenchymal compartments of the lacrimal gland.

In addition to MAPK, the class IA phosphoinositide 3-kinase (PI3K) is another major cell signaling regulator activated by FGF receptors and other receptor tyrosine kinases (RTKs) (*11*). Composed of a p85 regulatory subunit and a p110 catalytic subunit, PI3K may be recruited through SH2 domains of p85 or the Ras binding domain (RBD) of p110, respectively. The latter belies a direct cross-talk between PI3K and Ras signaling (*12*, *13*). Previous studies have shown that disruption of the Ras-PI3K interaction by mutating the RBD of p110α blocked Ras-driven tumorigenesis in the lung (*14*–*16*). Similarly, we also observed that the RBD-mediated signaling from Ras is necessary for the elevated PI3K-AKT activity in skin tumors caused by *Pten* deletion (*17*). Although both models have demonstrated that Ras promotes PI3K activity in vivo, whether PI3K also affects Ras signaling under the physiological condition remains unclear.

In this study, we used lacrimal gland development as a model to study the regulation and function of PI3K. We present evidence that genetic ablation of *p85* only partially disrupts PI3K activity during lacrimal gland development, whereas the RBD of p110 is specifically required for FGF to induce PI3K signaling. In contrast, loss of *p110* disrupts insulin-like growth factor (IGF) signaling and abolishes lacrimal gland budding. *p110* deletions also impair MAPK signaling, and the *p110*-mutant lacrimal gland phenotype can be partially reversed by active MAPK signaling, demonstrating that PI3K is required for MAPK activity in vivo. Our data further indicate that PI3K and extracellular signal–regulated kinase (ERK) jointly regulate mammalian target of rapamycin (mTOR) signaling in the lacrimal gland bud, which is in turn required for PI3K and MAPK activity. Last, we demonstrate that the PI3K-MAPK-mTOR signaling network prevents the expression of epidermal growth factor receptor (Egfr) in the lacrimal gland bud and increasing EGF signaling inhibits lacrimal gland budding. These results not only establish the reciprocal interactions among PI3K, Ras, and mTOR in vivo but also reveal that they control the spatial patterning of cell surface receptors to regulate budding morphogenesis.

[1]Departments of Ophthalmology, Pathology, and Cell Biology, Columbia University, New York, NY, USA. [2]Wuxi School of Medicine, Jiangnan University, Wuxi, China. [3]Department of Biochemistry, School of Basic Medicine, Jining Medical University, Jining, Shandong, China. [4]Department of Cancer Biology, Dana-Farber Cancer Institute, Boston, MA, USA.
*Corresponding author. Email: xz2369@columbia.edu
†These authors contributed equally to this work.
‡Present address: Department of Surgery, Indiana University School of Medicine, Indianapolis, IN 46202, USA.
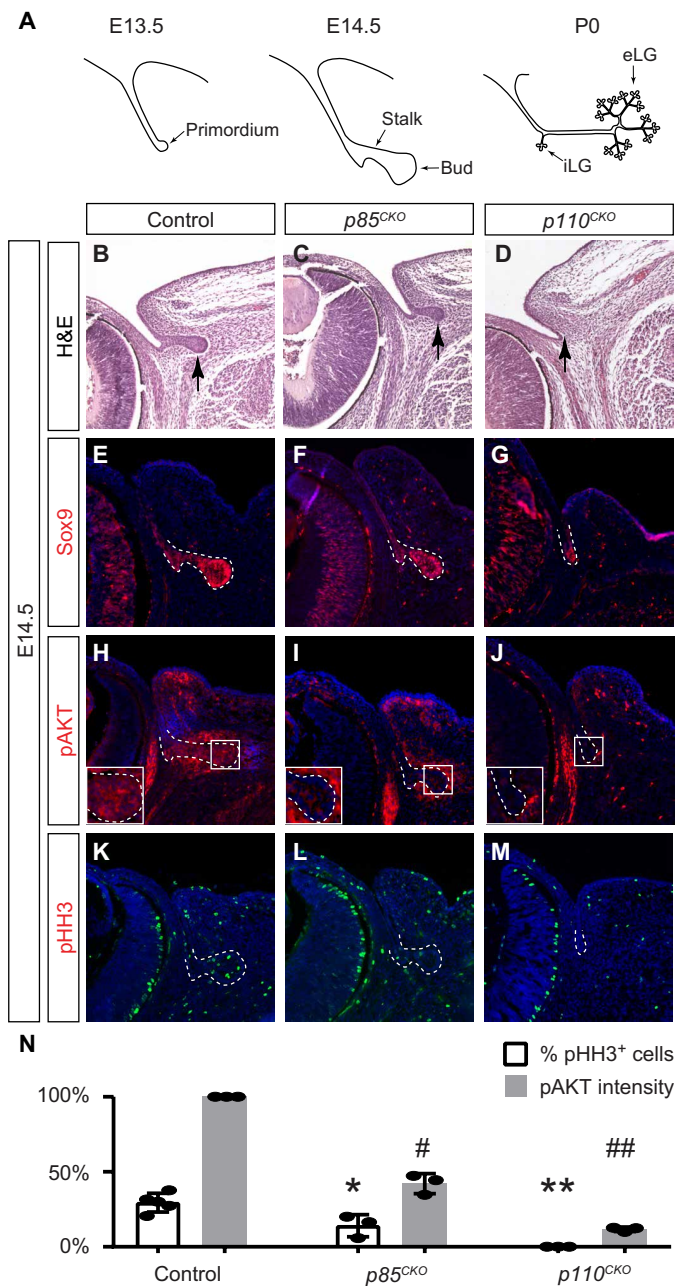
Fig. 1. PI3K signaling is required for lacrimal gland development. (**A**) The lacrimal gland primordium arises as thickening of the conjunctival epithelium at mouse embryonic day 13.5 (E13.5). One day later, it elongates to form a bud followed by an extended stalk. At postnatal day 0 (P0), the lacrimal gland is composed of two glandular structures with extensive branches. iLG, intraorbital lacrimal gland; eLG, extraorbital lacrimal gland. (**B** to **D**) Lacrimal gland buds (arrows) were presented at E14.5 in control and $p85^{CKO}$ mutants but not in $p110^{CKO}$ embryos. H&E, hematoxylin and eosin. (**E** to **J**) Although the progenitor cell marker Sox9 was preserved in the lacrimal gland primordia, pAKT was reduced in $p85^{CKO}$ and lost in $p110^{CKO}$ mutants. (**K** to **M**) Compared to controls, $p85^{CKO}$ and $p110^{CKO}$ mutants exhibited fewer or even no pHH3$^+$ cells, respectively. (**N**) Quantification of pHH3$^+$ cells and pAKT staining. One-way analysis of variance (ANOVA): $*P < 0.02$ for $p85^{CKO}$ versus control, $**P < 0.05$ for $p85^{CKO}$ versus $p110^{CKO}$, $\#P < 0.0001$ for $p85^{CKO}$ versus control, and $\#\#P = 0.0002$ for $p85^{CKO}$ versus $p110^{CKO}$. $n = 5$ for pHH3$^+$ quantification of controls and $n = 3$ for all other genotypes.

RESULTS

Both p85 and Ras regulate p110 activity in the lacrimal gland

To investigate the role of PI3K signaling in lacrimal gland development, we first used *Le-Cre* to generate a conditional knockout of the PI3K regulatory subunits p85α and p85β. *Le-Cre* is a bicistronic transgene expressing both Cre and green fluorescent protein (GFP) in the conjunctival and lacrimal gland epithelium (*7*). As revealed by the GFP reporter and histology, *Le-Cre;p85α$^{flox/flox}$;p85β$^{KO/KO}$* (*p85^{CKO}*)–mutant embryos still presented elongated lacrimal gland buds comparable to wild-type controls (Fig. 1, B and C, and fig. S1A). At P0 (postnatal day 0), however, whereas control lacrimal glands contained both intra- and extraorbital compartments (iLGs and eLGs) linked by a connecting duct, *p85^{CKO}* mutants displayed only residual iLGs close to the eye (fig. S1A, arrows). We next ablated the PI3K catalytic subunit p110α and p110β to determine the full extent of PI3K function in lacrimal gland development. *Le-Cre;p110α$^{flox/flox}$* mutants exhibited residual lacrimal gland buds at E14.5 (embryonic day 14.5), whereas *Le-Cre;p110β$^{flox/flox}$* mutants only showed slight reduction in the lacrimal gland length (fig. S1B). In contrast, lacrimal gland development was completely blocked in *Le-cre;p110α$^{flox/flox}$;p110β$^{flox/flox}$* (*p110^{CKO}*) mutants (Fig. 1D and fig. S1A, arrows). These results demonstrated that PI3K is essential for lacrimal gland development.

We next sought to understand the molecular basis of the phenotype disparity between the *p85^{CKO}* and *p110^{CKO}* mutants. At E14.5, Sox9 (SRY-Box Transcription Factor 9) marked the lacrimal gland buds in both control and *p85^{CKO}* embryos (Fig. 1, E and F) (*18*). Although there was no lacrimal gland bud in E14.5 *p110^{CKO}* mutants, Sox9 expression was present in the fornix of the conjunctiva (Fig. 1G), suggesting that the lacrimal progenitor cells were still preserved. In addition, the expression of *Fgf10* in the periocular mesenchyme was unchanged in *p110^{CKO}* mutants, confirming that this main inductive signal for the lacrimal gland budding was unaffected (fig. S1C, arrows). In contrast, phospho-AKT (pAKT) staining was diminished in *p85^{CKO}* mutant lacrimal glands in comparison to controls, and it was further reduced in *p110^{CKO}* mutants (Fig. 1, H to J and N). pAKT was also down-regulated in the periocular mesenchyme surrounding the lacrimal gland bud, suggesting an intricate interaction between these two tissue compartments. Consistent with the role of PI3K-AKT signaling in cell proliferation, the number of phospho-histone3–positive (pHH3$^+$) mitotic cells was reduced in *p85^{CKO}* lacrimal gland buds and further eliminated in *p110^{CKO}* mutants (Fig. 1, K to N). Thus, PI3K signaling is progressively disrupted by *p85* and *p110* deletions.

Because PI3K signaling was reduced to different extents in *p110* and *p85* mutants, we reasoned that p110 must have an alternative mode of activation during lacrimal gland development (Fig. 2A). One potential candidate is FGF signaling, which is active in the lacrimal gland bud. Although previous in vitro studies have suggested that FGF can elicit PI3K signaling using the adaptor protein Gab1 (GRB2 Associated Binding Protein 1) to recruit p85, we have shown in mouse embryonic fibroblast (MEF) cells that Gab1 is dispensable for FGF to activate PI3K-AKT signaling (*19, 20*). We did not observe any lacrimal gland phenotype in 2-month-old *Le-cre;Gab1$^{flox/flox}$* (*Gab1^{CKO}*) animals (fig. S2). On the other hand, it has also been shown that FGF can promote PI3K signaling via Ras, which is known to interact with p110α directly (*14*). We confirmed this finding in MEF cells carrying two point mutations in the RBD of p110α (*p110α$^{RBD/RBD}$*). In contrast to control MEF cells that displayed significant increase in pAKT after addition of FGF, the FGF-induced AKT phosphorylation was lost in *p110α$^{RBD/RBD}$* cells (Fig. 2B). We next generated *Le-Cre;p110α$^{flox/RBD}$;p110β$^{flox/flox}$*
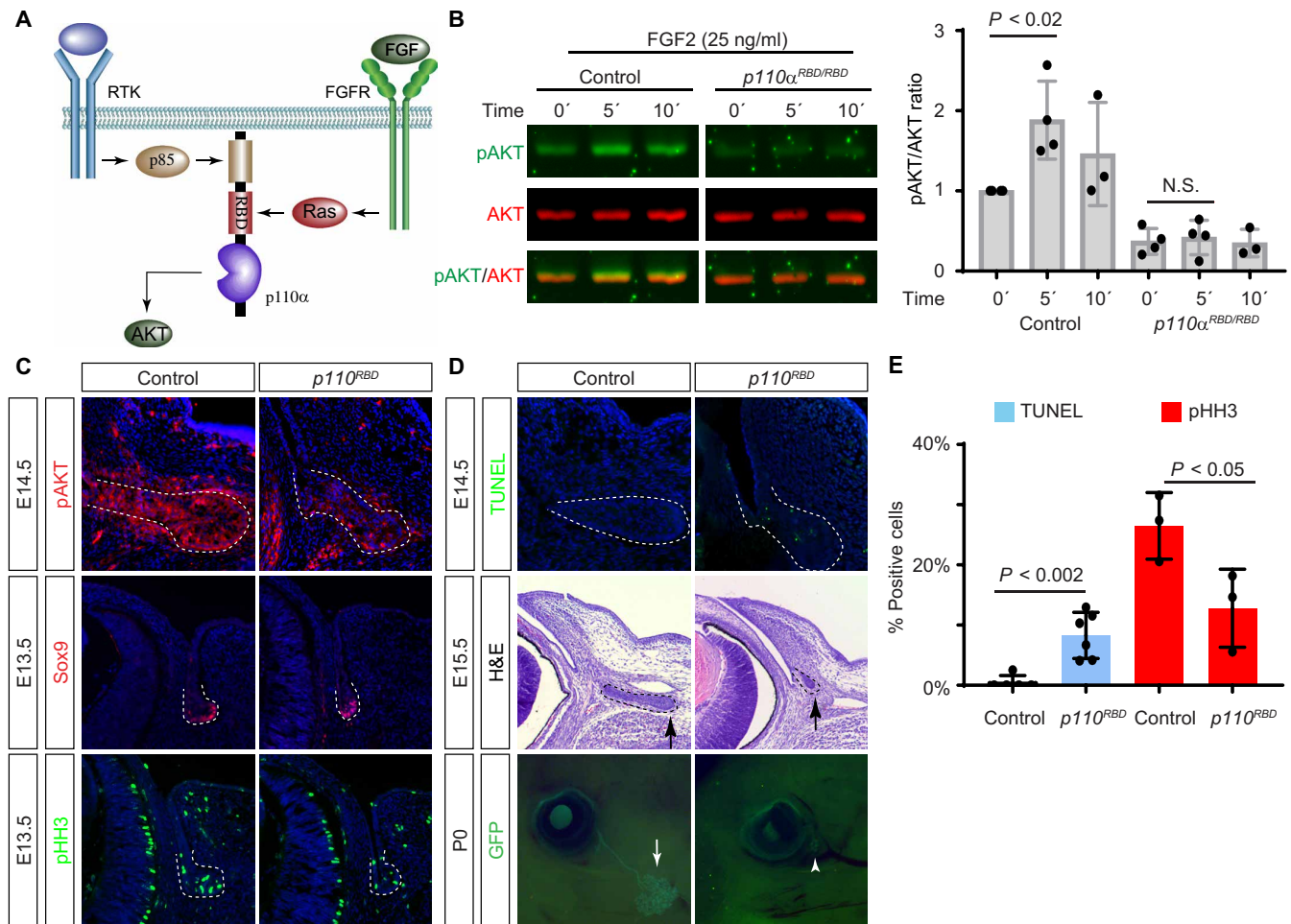
Fig. 2. The p110α-Ras interaction is required for FGF to activate PI3K signaling. (**A**) Schematic diagram of PI3K activation. The p110α catalytic subunit of PI3K can be stimulated by RTK via binding to p85, or it could be coupled to FGF signaling via interaction with Ras. (**B**) FGF2 treatment led to increased levels of pAKT in control but not in $p110\alpha^{RBD/RBD}$ MEF cells that carry mutations disrupting the p110α RBD domain. One-way ANOVA was used to test for statistical significance ($n = 4$ for data at 0′ and 5′ and $n = 3$ for data at 10′). N.S., not significant. (**C** and **D**) $p110^{RBD}$ mutants still expressed Sox9 in lacrimal gland buds but exhibited reduced staining for both pAKT and pHH3, while TUNEL staining was increased. The lacrimal glands were much reduced in $p110^{RBD}$ mutants at E15.5 and birth. (**E**) Quantification of pHH3 ($n = 6$)– and TUNEL ($n = 3$)–positive cells. Student's t test was used to calculate statistical significance.

($p110^{RBD}$) animals to block the Ras-p110α interaction during lacrimal gland development. As expected, we found that phosphorylation of AKT in lacrimal gland buds was attenuated in E14.5 $p110^{RBD}$ embryos as compared to controls (Fig. 2C). As a result, although Sox9 was still expressed in $p110^{RBD}$-mutant lacrimal gland buds, there was a significant decrease in cell proliferation as indicated by pHH3 staining and a drastic increase in cell apoptosis as revealed by terminal deoxynucleotidyl transferase–mediated deoxyuridine triphosphate nick end labeling (TUNEL) assay (Fig. 2, C to E). Similar to $p85^{CKO}$ mutants, $p110^{RBD}$ animals also exhibited smaller lacrimal gland buds at E15.5 and hypoplastic lacrimal glands at P0 (Fig. 2D, arrow and arrowhead). Together, our data showed that the PI3K activity in the lacrimal gland bud requires both RTK signaling mediated by p85 and FGF signaling mediated by the Ras-p110α interaction.

p110 is required for PI3K and MAPK signaling during lacrimal gland development

We next explored the downstream targets of PI3K in lacrimal gland development by transcriptomic analysis. The lacrimal gland epithelial tissues were collected from E14.5 control (*Le-Cre*), $p110^{RBD}$, and $p110^{CKO}$ embryos by microdissection using laser capture microscopy ($n = 3$ for each condition) and subjected to RNA sequencing (RNA-seq) as previously described (*21*). Unsupervised clustering analysis using the top 100 most variable genes showed that these samples were segregated into three discrete groups, demonstrating the consistency of our preparations (Fig. 3A). Furthermore, the gene expression profiles exhibited orderly transitions from control, $p110^{RBD}$ to $p110^{CKO}$ mutants, corresponding to the worsening of the lacrimal gland phenotypes. As expected, from the biochemical function of p110, these differentially expressed genes are enriched in gene ontology (GO) terms such as PI3K-AKT signaling and inositol phosphate metabolism (Fig. 3B). Moreover, GO analysis indicated that cell cycle, carbon metabolism, and glycolysis were also affected, consistent with the known role of PI3K in cell growth and metabolism. A major RTK pathway targeting PI3K and cell metabolism is IGF signaling, whose ligands (Igf1 and Igf2) and receptors (Igfr1 and Igfr2) are expressed in the lacrimal gland region (fig. S3). Gene set enrichment analysis (GSEA) showed that $p110$ deletion disrupted
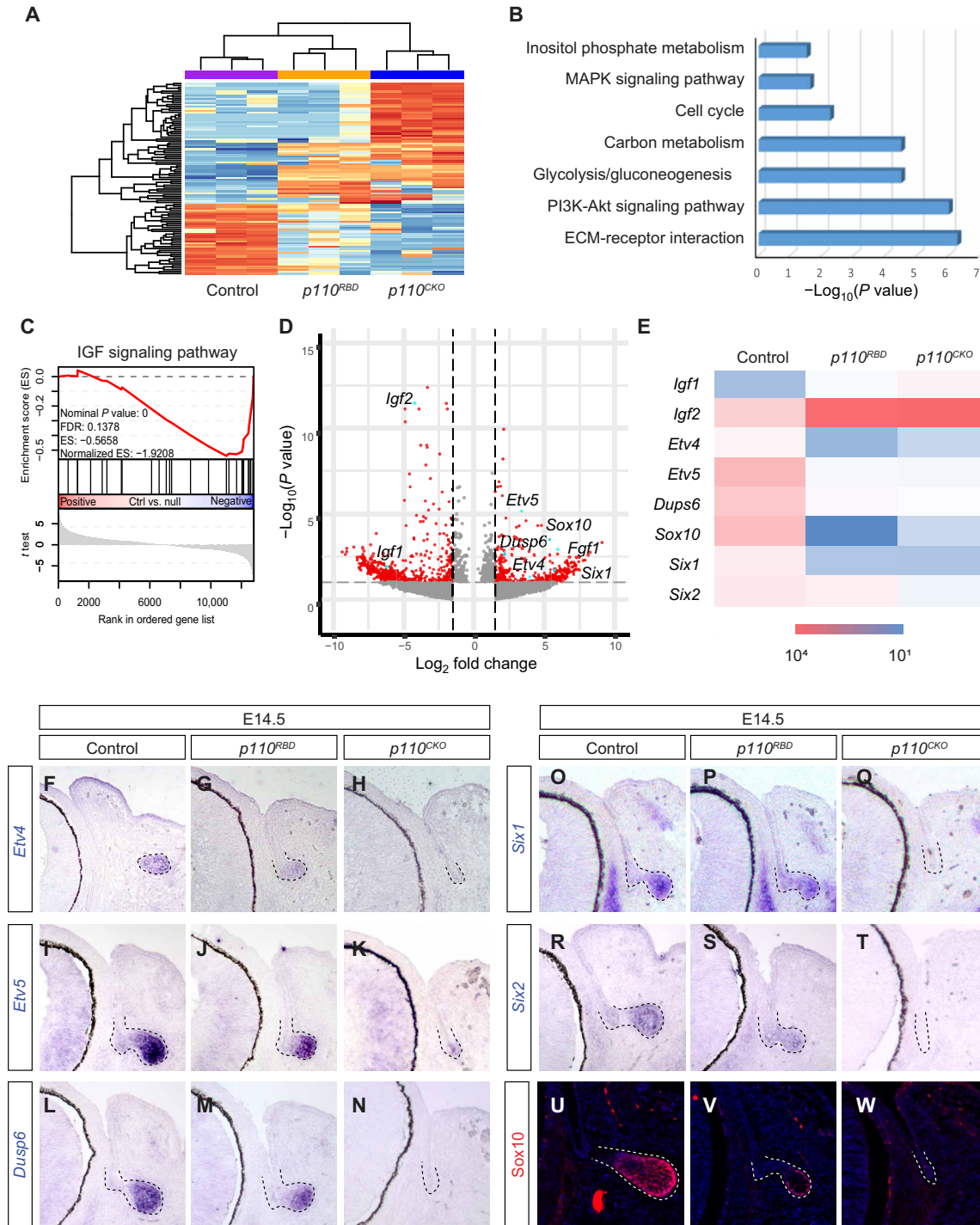
Fig. 3. *p110* mutations disrupt PI3K signaling and expression of MAPK response genes. (**A**) Segregation of E14.5 control, *p110^RBD^*, and *p110^CKO^* lacrimal gland transcriptomes shown by cluster analysis. (**B**) GO analysis showed that the differentially regulated genes in *p110^CKO^* mutants were enriched in PI3K-regulated pathways. ECM, extracellular matrix. (**C**) GSEA revealed that IGF signaling was disrupted in *p110^CKO^* mutants. FDR, false discovery rate. (**D**) As shown in volcano plot of the control versus the *p110^CKO^* transcriptome, *Igf1* and *Igf2* were among up-regulated genes, and *Fgf1*, *Etv4*, *Etv5*, *Dusp6*, *Six1*, and *Sox10* were significantly down-regulated. (**E**) Heatmap of differentially regulated genes implicated in IGF and MAPK pathways. (**F** to **W**) RNA in situ hybridization and immunostaining confirmed down-regulation of MAPK response genes in *p110^RBD^* and *p110^CKO^* mutants.

IGF signaling (Fig. 3C). The volcano plot revealed that *Igf2* and, to the less extent, *Igf1* were among the most significantly up-regulated genes in $p110^{CKO}$ mutants, whereas *Fgf1* expression was greatly reduced (Fig. 3D). Therefore, loss of PI3K results in dysregulation of RTK signaling during lacrimal gland development.

An unexpected finding from the transcriptomic analysis is that MAPK signaling was also affected in $p110^{CKO}$ mutants (Fig. 3B). Several known MAPK responsive genes were progressively down-regulated in $p110^{RBD}$ and $p110^{CKO}$ mutants (Fig. 3, B and E). These include *Etv4* and *Etv5*, which encode ETS (E-twenty six) domain transcription factors important for lacrimal gland cell fate determination (8). RNA in situ hybridization experiments confirmed that *Etv4* and *Etv5* were specifically expressed in the control lacrimal gland buds but attenuated in $p110^{RBD}$ and greatly diminished in $p110^{CKO}$ mutants (Fig. 3, F to K). Dusp6 (Dual-specificity phosphatase 6) is a dual specificity MAPK phosphatase frequently induced in the region of active MAPK signaling. In $p110^{RBD}$ and $p110^{CKO}$ mutants, *Dusp6* expression was either reduced or absent (Fig. 3, L to N). *Six1*, *Six2*, and *Sox10* are also known targets of MAPK signaling important for branching morphogenesis of the lacrimal gland (8). Their expressions were similarly blocked by genetic ablation of *p110* (Fig. 3, O to W). Considering the importance of these MAPK-dependent genes in lacrimal gland development, these observations suggested that dysregulation of MAPK signaling contributes significantly to the *p110* lacrimal gland phenotype.

PI3K activates MAPK signaling to promote lacrimal gland budding

To explore the mechanism by which PI3K regulates MAPK activity, we first considered Rac1 (Ras-related C3 botulinum toxin substrate 1), which has been shown to act downstream to PI3K to promote MAPK signaling in cancer cells (22). However, genetic ablation of *Rac1* did not produce any lacrimal gland phenotype in adult *Le-cre;Rac1^{flox/flox}* animals (fig. S4), which ruled out Rac1 as a significant regulator of MAPK signaling. On the other hand, since the RBD of p110α is required for PI3K activation by Ras after FGF stimulation, we asked whether this domain may also mediate the activation of Ras by PI3K. As shown in Fig. 4A, FGF2 induced both ERK and AKT phosphorylation in control MEF cells. In $p110α^{RBD/RBD}$ MEF cells, however, not only was pAKT activation abolished, but there was also significant reduction in the level of pERK. We further performed Ras pull-down assay to measure the ratio of active Ras versus total Ras. Consistent with the lower Ras activity, the proportion of the guanosine 5′-triphosphate (GTP)–bound form of Ras (Ras-GTP) was also reduced in $p110α^{RBD/RBD}$ MEF cells compared to the control (Fig. 4A). In addition, although the FGF-induced pERK and pAKT were unaffected after ablation of p85, the IGF-induced pERK and pAKT were down-regulated in both *p85* knockout and $p110α^{RBD/RBD}$ MEF cells (fig. S5, A to C). Last, combined deletion of both p110α and p110β resulted in drastic loss of both pAKT and pERK (Fig. 4B). These results showed that p110 proteins are required for FGF and IGF to stimulate MAPK.

To confirm the role of PI3K in MAPK activation in vivo, we next examined ERK phosphorylation during lacrimal gland development. At E14.5, pERK was restricted to lacrimal gland buds in control embryos (Fig. 4C), but the staining was reduced in both $p85^{CKO}$ and $p110^{RBD}$ lacrimal glands and greatly diminished in $p110^{CKO}$ mutants (Fig. 4C and fig. S5D). We reasoned that, if MAPK is a functional target of PI3K, constitutively active MAPK may ameliorate

lacrimal gland phenotypes in *p110* mutants. To test this hypothesis, we took advantage of a Cre-inducible allele, $R26R\text{-}LSL\text{-}Mek1^{DD}$, to express a mitogen-activated protein kinase kinase 1 (Mek1) variant (Mek1^{DD}) that can phosphorylate ERK in the absence of upstream stimulation (23). In *Le-cre;p110α^{flox/flox}*, $p110β^{flox/flox}$, $R26R\text{-}LSL\text{-}Mek1^{DD}$ ($p110^{CKO}$;Mek1^{DD}) mutants, we observed an increase in pERK staining compared to $p110^{CKO}$ mutants (Fig. 4C). Whereas lacrimal gland development was aborted in $p110^{CKO}$ embryos, lacrimal gland buds were observed in $p110^{CKO}$;Mek1^{DD} mutants. At birth, both control (*Le-Cre*) and Mek1^{DD} (*Le-Cre;Mek1^{DD}*) pups displayed extensively branched iLG and eLG, whereas mostly residual iLGs were present in $p110^{RBD}$ animals (Fig. 4D, arrows and arrowheads). In contrast, *Le-cre;p110α^{flox/RBD}*, $p110β^{flox/flox}$, $R26R\text{-}LSL\text{-}Mek1^{DD}$ ($p110^{RBD}$;Mek1^{DD}) mutants predominantly had stunted eLG and sometimes even intact lacrimal glands. Similarly, although $p110^{CKO}$ pups lacked either iLG or eLG, 50% of $p110^{CKO}$;Mek1^{DD} mutants presented residual lacrimal glands. These genetic rescue experiments provided strong support that MAPK activation by PI3K is important for lacrimal gland development.

MAPK and PI3K converge upon mTOR signaling

mTOR is a well-known effector of the PI3K/AKT pathway (24). In control E14.5 lacrimal gland buds, we observed strong phosphorylation of mTOR and two of its downstream targets, 4EBP1 [eukaryotic translation initiation factor 4E (eIF4E)–binding protein 1] and S6 (Fig. 5, A, E, and I). Consistent with the role of PI3K in mTOR regulation, these staining weakened in both $p85^{CKO}$ and $p110^{RBD}$ lacrimal glands (Fig. 5, B, C, F, G, J, and K). In $p110^{CKO}$ mutants, however, although p4EBP1 and pS6 were lost, there was still residual pmTOR staining (Fig. 5, D, H and L), suggesting that inactivation of PI3K does not completely abolish mTOR signaling.

Previous studies have suggested that Wnt and MAPK signaling may also regulate mTOR, although the in vivo evidence is lacking (25, 26). To test these two candidates, we first generated a lacrimal gland specific knockout of Lrp5 (LDL Receptor Related Protein 5) and Lrp6, two obligatory receptors of the canonical Wnt signaling. Although *Le-cre;Lrp5^{flox/flox}*, $Lrp6^{flox/flox}$ (Lrp^{CKO}) mutants lacked lacrimal gland buds at E14.5, there were still lacrimal gland progenitor cells marked by Sox9 expression in the conjunctiva (Fig. 5, M and N). These cells displayed pERK and pmTOR staining comparable to those in control lacrimal gland buds (Fig. 5, P, Q, S, and T), demonstrating that Wnt signaling was dispensable for mTOR activity. We next ablated the two MAPKs, Erk1 and Erk2. In *Le-cre;Erk1^{−/−};Erk2^{flox/flox}* (Erk^{CKO}) embryos, not only was pERK lost, but pmTOR staining was also greatly diminished (Fig. 5, O, R, and U). Together, these results showed that MAPK, but not Wnt signaling, is required for mTOR signaling during lacrimal gland development.

The partial reduction of pmTOR in either $p110^{CKO}$ or Erk^{CKO} mutants raised the possibility that PI3K and MAPK may cooperate to regulate mTOR activity. We tested this hypothesis in MEF cells using pharmacological inhibitors. In control cells treated with dimethyl sulfoxide (DMSO), there was active mTOR signaling as indicated by the phosphorylation of mTOR and 4EBP1 (Fig. 5V). Treatment with PI3K inhibitor LY294002 abolished the AKT phosphorylation as expected, and it also partially reduced the level of pERK, consistent with our early results that MAPK signaling was dependent on PI3K activity. In agreement with in vivo findings, inhibition of PI3K by LY294002 blocked phosphorylation of 4EBP1 but left pmTOR at a reduced level. On the other hand, the MEK
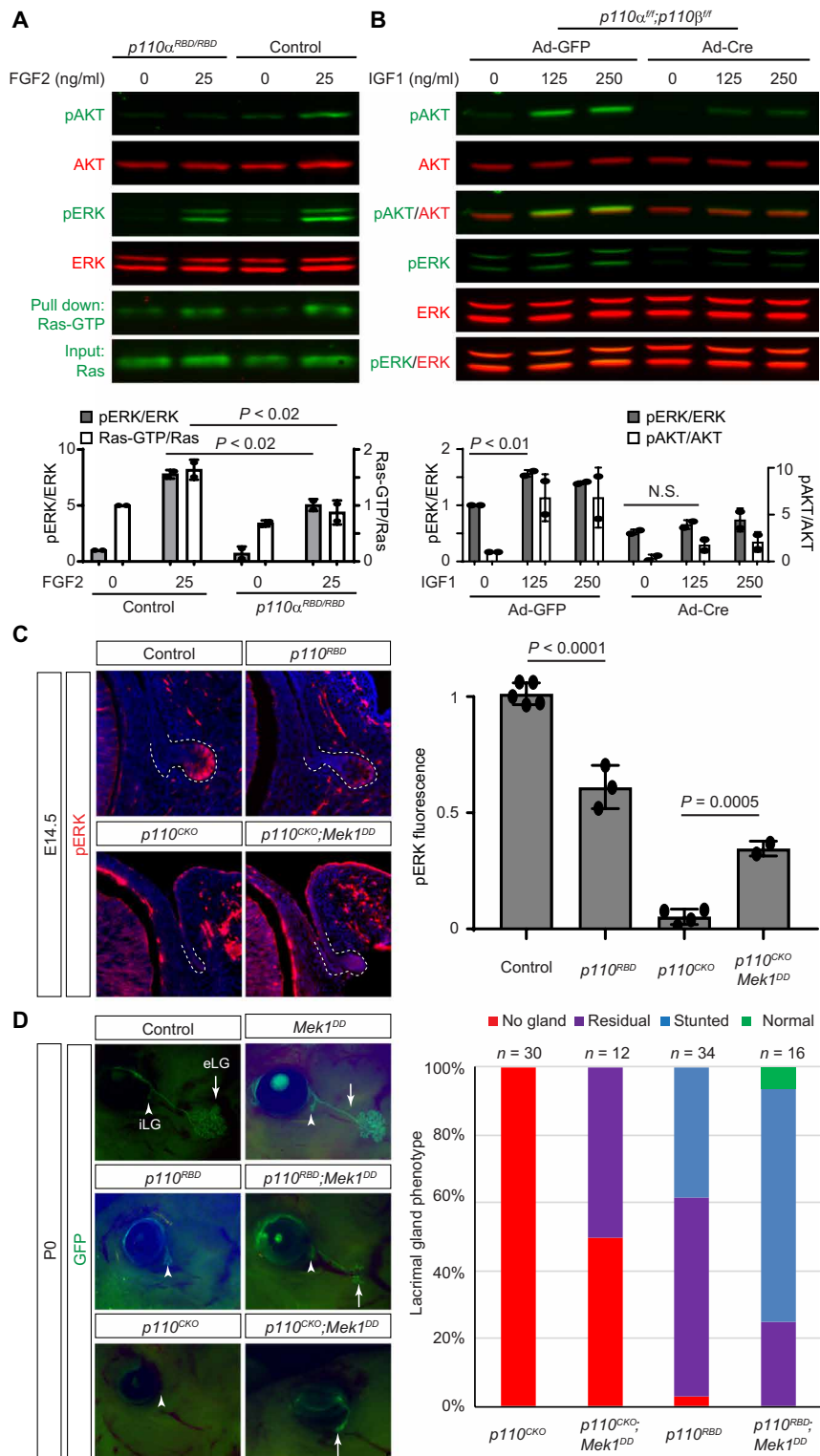
Fig. 4. PI3K activates MAPK via the p110α-Ras interaction. (**A**) In $p110\alpha^{RBD/RBD}$ MEF cells, the loss of the p110α-Ras interaction not only prevented FGF from inducing AKT phosphorylation but also down-regulated the levels of pERK and active Ras (Ras-GTP). One-way ANOVA test for statistical significance ($n = 2$). (**B**) Deletion of $p110\alpha$ and $p110\beta$ in MEF cells disrupted IGF-induced AKT and ERK phosphorylation. One-way ANOVA test for statistical significance ($n = 2$). (**C**) pERK staining was down-regulated in $p110^{RBD}$ glands and sharply reduced in $p110^{CKO}$ mutants. Expression of the constitutively active $Mek1^{DD}$ allele led to partial recovery of lacrimal gland budding and pERK staining in $p110^{CKO};Mek1^{DD}$ mutants. One-way ANOVA test ($n = 5$ for the control and $n = 3$ for the rest). (**D**) In comparison to control and $Mek1^{DD}$ pups, $p110^{RBD}$ mutants mostly displayed residual glands at birth, whereas $p110^{RBD};Mek1^{DD}$ animals showed more extensively branched glands. Similarly, lacrimal gland induction was observed in $p110^{CKO};Mek1^{DD}$ mutants but not in $p110^{CKO}$ mutants.
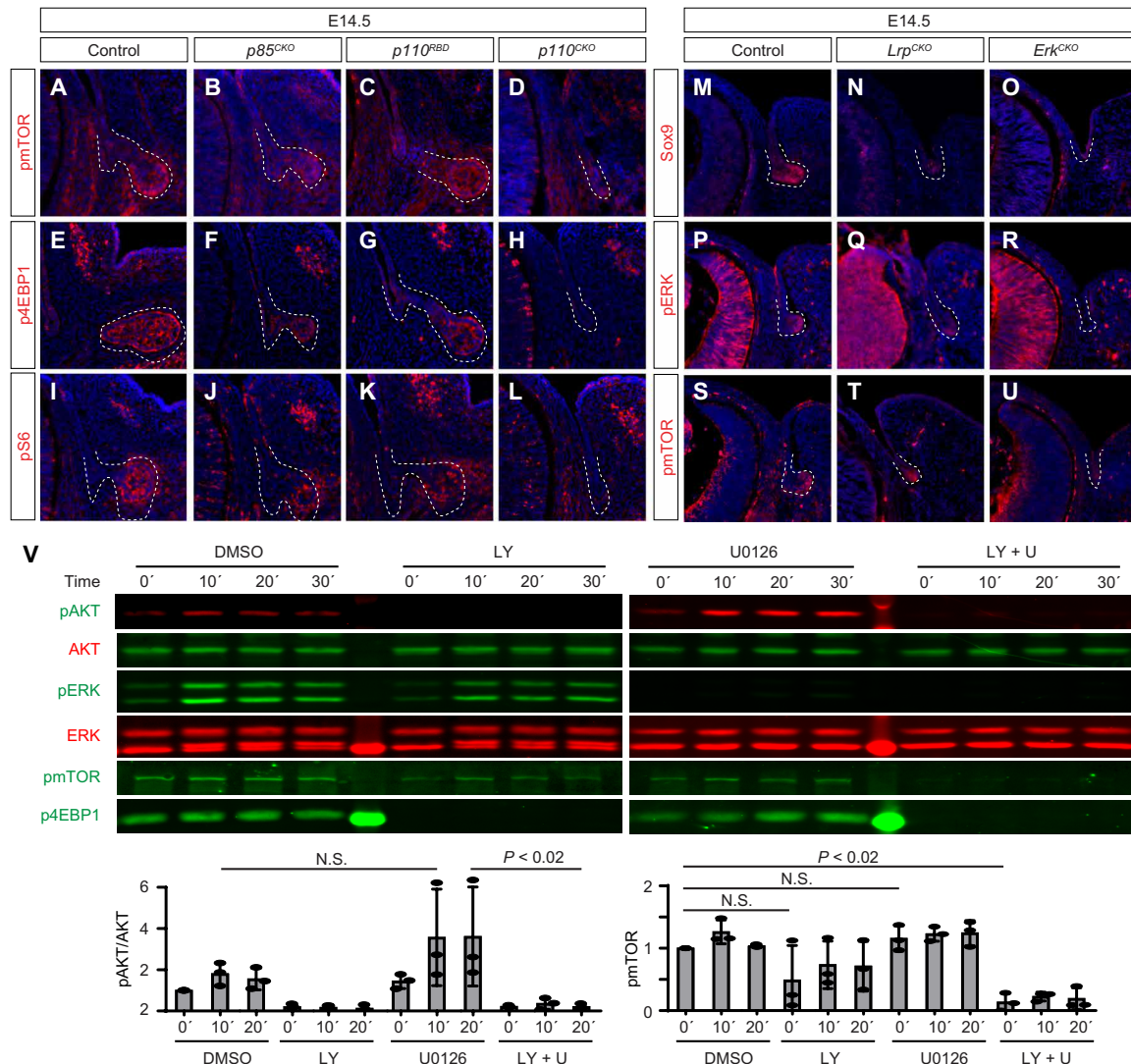
Fig. 5. ERK cooperates with PI3K to control mTOR activity. (**A** to **L**) pmTOR, p4EBP1, and pS6 were reduced in $p85^{CKO}$ and $p110^{RBD}$ lacrimal gland buds. In $p110^{CKO}$ mutants, however, there was persistent pmTOR staining despite loss of p4EBP1 and pS6. (**M** to **U**) Although Lrp^{CKO} mutants lacked lacrimal gland buds, they retained pERK and pmTOR staining in the Sox9-positive progenitor cells. Erk^{CKO} mutants also preserved Sox9 expression, but the pERK staining was lost, and pmTOR was diminished. (**V**) In MEF cells treated with FGF2 (25 ng/ml), PI3K inhibitor LY294002 (LY) abolished induction of pAKT, but pERK and pmTOR were only partially reduced. MEK inhibitor U0126 (U) only abrogated pERK induction. In contrast, combined treatment of PI3K and MEK inhibitors (LY + U) abolished mTOR phosphorylation. One-way ANOVA test ($n = 3$).

inhibitor U0126 abrogated ERK phosphorylation and reduced pmTOR similar to LY294002 treatment. Only in the presence of both PI3K and ERK inhibitors was phosphorylation of mTOR completely abolished. This result was corroborated using another PI3K inhibitor PX866 (fig. S6), demonstrating that PI3K and MAPK signaling functions cooperatively regulate mTOR signaling.

mTORC1 controls AKT and MAPK signaling during lacrimal gland development

mTOR can form two multiprotein complexes, mTORC1 and mTORC2, which are distinguished by their respective subunits, Raptor and Rictor (24). To determine which complex is required for lacrimal gland development, we examined conditional knockout mutants targeting these two critical partners of mTOR. At E14.5, Le-$cre;Rictor^{flox/flox}$ ($Rictor^{CKO}$) mutants have formed lacrimal gland buds expressing the progenitor cell marker Sox9, but the Sox9+ cells in Le-$cre;Raptor^{flox/flox}$

($Raptor^{CKO}$) embryos were still confined to the conjunctiva (Fig. 6, A to C). Unlike those in $Rictor^{CKO}$ mutants, these $Raptor$-deficient cells not only lacked p4EBP1 and pS6 but also lost pmTOR staining (Fig. 6, D to L), suggesting an auto regulatory mechanism by which mTORC1 regulates its own activity. In $Raptor^{CKO}$ mutants, we also failed to observe expression of Sox10 (Fig. 6, M to O), which we have previously showed to be downstream to MAPK signaling (8). In line with this finding, mTOR inhibitor Torin not only abolished phosphorylation of AKT and mTOR in MEF cells but also prevented FGF from inducing ERK phosphorylation (Fig. 6P). This result was further confirmed in vivo, where pERK staining was significantly down-regulated in $Raptor^{CKO}$ mutants (Fig. 6, Q and R). These data showed that mTORC1 is required for both AKT and MAPK signaling.

The results so far have revealed the mutual dependency between MAPK and mTORC1 signaling. Thus, we investigated whether elevation of one pathway was able to rescue lacrimal gland defects
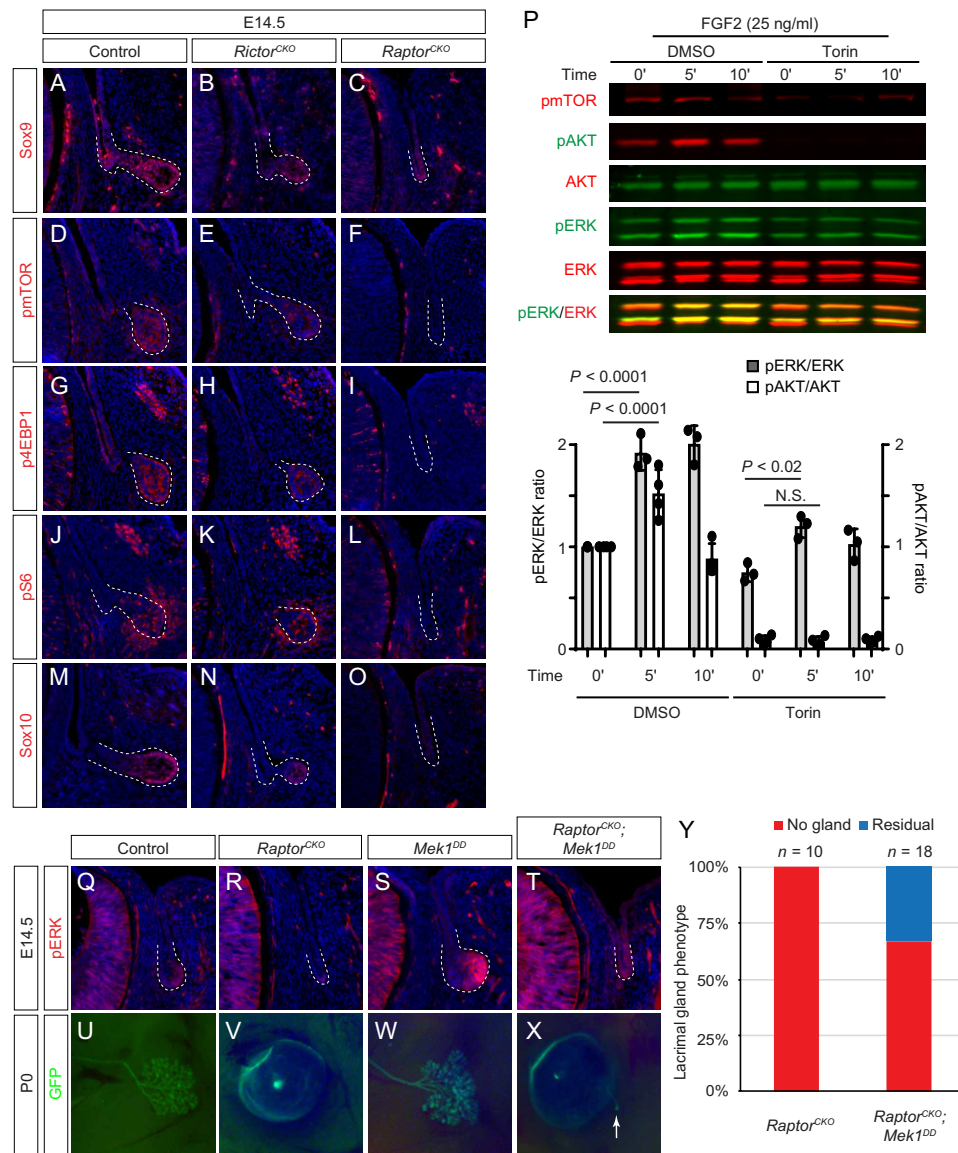
Fig. 6. mTORC1 is required for lacrimal gland budding and ERK phosphorylation. (**A** to **L**) Although deletion of the mTORC2 subunit *Rictor* did not affect lacrimal gland budding in *Rictor*[CKO] embryos, loss of the mTORC1 subunit Raptor in *Raptor*[CKO] mutants resulted in loss of pmTOR, p4EBP1, and pS6 in Sox9-expressing progenitor cells. (**M** to **O**) The expression of Sox10 was also lost in *Raptor*[CKO] mutants. (**P**) The mTOR inhibitor Torin not only abolished FGF-induced phosphorylation of mTOR and AKT but also down-regulated the level of pERK. The statistical significance was calculated using one-way ANOVA test ($n = 3$ for pERK and $n = 4$ for pAKT). (**Q** to **X**) pERK staining was reduced in *Raptor*[CKO] mutants, elevated in *Mek1*[DD], and partially recovered in *Raptor*[CKO];*Mek1*[DD] embryos. As a result, although *Raptor*[CKO] mutants lacked any lacrimal gland, residual lacrimal gland was observed in *Raptor*[CKO];*Mek1*[DD] pups. (**Y**) Quantification of lacrimal gland phenotypes.

caused by the loss of the other. Tuberous Sclerosis Complex 1 (Tsc1) is a negative regulator of mTORC1 (*24*). As shown by increasing pmTOR and pS6 staining in *Le-cre;Tsc1*[flox/flox] (*Tsc1*[CKO]) mutants (fig. S7A), deletion of *Tsc1* resulted in up-regulation of mTORC1 activity. However, neither *Erk*[CKO] ($n = 16$) nor *Le-cre;Erk1*^{−/−}*;Erk2*[flox/flox]; *Tsc1*[flox/flox] (*Erk*[CKO]*;Tsc1*[CKO]; $n = 8$) mutants displayed any lacrimal gland at P0 (fig. S7B), indicating that the removal of the mTORC1 suppressor alone was unable to compensate for the loss of MAPK signaling during lacrimal gland development. In contrast, we observed that expression of *Mek1*[DD] led to significance increase in pERK staining in E14.5 *Le-cre;R26R-LSL-Mek1*[DD] (*Mek1*[DD]) and *Le-cre;Raptor*[flox/flox]*, R26R-LSL-Mek1*[DD] (*Raptor*[CKO]*;Mek1*[DD]) embryos

compared to the control and *Raptor*[CKO], respectively (Fig. 6, S and T). As a result, although lacrimal gland was absent in *Raptor*[CKO] pups, 40% of *Raptor*[CKO];*Mek1*[DD] mutants presented residual lacrimal gland at birth (Fig. 6, U to Y). Therefore, increasing MAPK signaling can partially restore lacrimal gland induction in the absence of mTORC1 signaling.

PI3K and mTORC1 suppressed aberrant EGF signaling detrimental to lacrimal gland budding

In addition to the down-regulated genes in *p110* mutants, our transcriptomic analysis also showed that many genes were up-regulated. Among them was *Egfr*, whose expression was progressively elevated
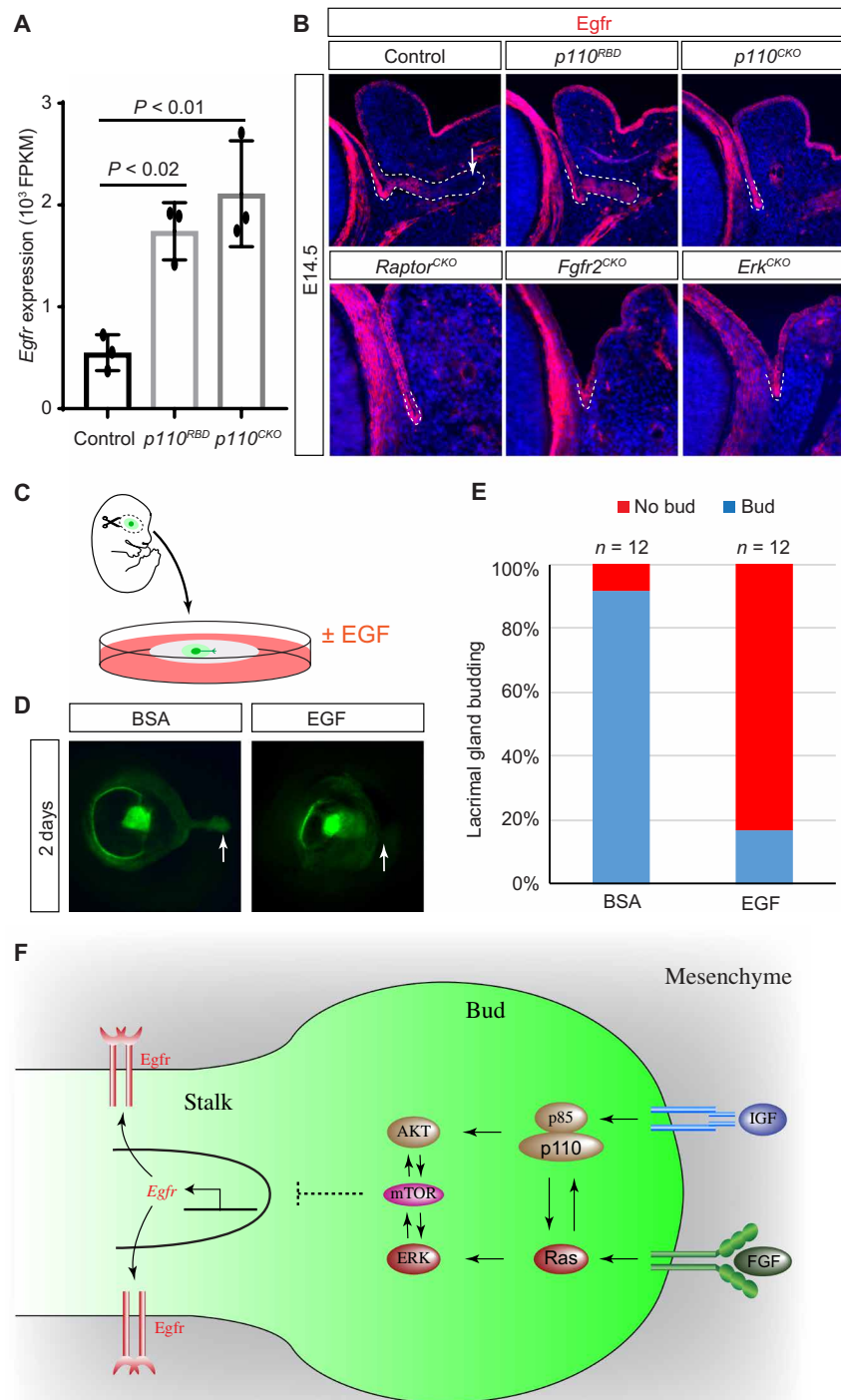
Fig. 7. Suppression of EGF signaling by PI3K and MAPK is necessary for lacrimal gland budding. (**A**) *Egfr* expression obtained by RNA-seq analysis was elevated in *p110RBD* and *p110CKO* mutants. FPKM, Fragments Per Kilobase of transcript per Million. (**B**) In control lacrimal glands, Egfr was expressed in the stalk region but excluded from the bud. This distinction was lost in *p110RBD* lacrimal glands. In *p110CKO*, *Fgfr2CKO*, *ErkCKO*, and *RaptorCKO* mutants, Egfr was uniformly expressed in the conjunctiva. (**C**) The explant assay was performed with the eye tissue dissected from E13.5 *Le-Cre* embryos that expressed GFP. After cultured on the floating membrane in the presence or absence of EGF, the eye rudiment was evaluated for formation of the GFP⁺ lacrimal gland bud. (**D**) In 2 days of culture, the lacrimal gland budding was inhibited by EGF (100 ng/ml) but not bovine serum albumin (BSA). (**E**) Quantification of lacrimal gland budding. Fisher's exact test, $P = 0.0006$. (**F**) Model of PI3K-MAPK interaction in lacrimal gland development. The p110 subunit of PI3K is activated by both p85-mediated IGF signaling and Ras-mediated FGF signaling. Conversely, the p110α-Ras interaction also activates Ras to stimulate MAPK signaling, which cooperates with AKT to control mTOR activity. We propose that these signaling pathways may suppress Egfr expression (dashed lines), allowing the budding of the lacrimal gland from the conjunctiva.

from $p110^{RBD}$ to $p110^{CKO}$ mutants (Fig. 7A). This drew our attention because EGF signaling is known to play an important role in epidermal proliferation and differentiation (*27*). Immunostaining showed that Egfr was expressed in the E14.5 conjunctival epithelia, stronger in the bulbar conjunctiva adjacent to the developing cornea than that in the palpebral conjunctiva on the other side of the fornix (Fig. 7B). Egfr expression was restricted to the stalk of the developing lacrimal gland but excluded from the distal bud region marked by Sox10 (Fig. 7B and fig. S8A, arrows). This differential expression pattern disappeared in $p110^{RBD}$ mutants, where Egfr expression was extended to the entire lacrimal gland primordia. Moreover, $p110^{CKO}$ and $Raptor^{CKO}$ mutants expressed uniform levels of Egfr from the bulbar to the palpebral conjunctiva, including the fornix where the lacrimal gland progenitor cells reside. Similar pattern of Egfr expression was also observed in Le-cre;$Fgfr2^{flox/flox}$ ($Fgfr2^{CKO}$) and Erk^{CKO} mutants (Fig. 7B). In $p110^{RBD}$;$Mek1^{DD}$ and $p110^{CKO}$;$Mek1^{DD}$ mutants where lacrimal gland induction was partially rescued, Egfr expression was reduced in distal lacrimal gland buds (fig. S8A). Therefore, deficient FGF-PI3K-MAPK-mTOR signaling may lead to dysregulation of Egfr during lacrimal gland development.

The lack of Egfr expression in the distal lacrimal gland region suggested that EGF signaling may be a negative regulator of lacrimal gland budding. To test this hypothesis, we performed explants cultures to investigate whether increasing EGF signaling affects budding morphogenesis of the lacrimal gland. To this end, ocular tissues including the periocular mesenchyme were dissected from E13.5 embryos and placed on floating membranes to maintain the air-liquid interface as previously described (Fig. 7C) (*28*). These embryos carried the *Le-Cre* transgene that coexpresses a GFP reporter, which allowed us to visualize development of lacrimal glands. Since we included the periocular mesenchyme that secreted the endogenous Fgf10, ocular explants spontaneously sprouted lacrimal gland buds after placed in culture for 2 days. As expected, these buds were blocked by inhibitors against IGFR, PI3K, and mTOR, confirming the important role of these signaling in lacrimal gland budding (fig. S9). Addition of EGF also suppressed the budding of lacrimal gland buds in the ocular explants (Fig. 7, D and E). These results showed that up-regulation of EGF signaling is inhibitive for lacrimal gland budding.

DISCUSSION
In this study, we systematically explored the regulation and function of PI3K signaling in lacrimal gland development (Fig. 7F). Our results show that the PI3K catalytic subunit p110 is partially controlled by the regulatory subunit p85, which can be activated by IGF signaling. On the other hand, p110α interacts with Ras to mediate the FGF-induced PI3K signaling. We present biochemical and genetic evidence that the p110α-Ras interaction is also required for Ras activity, establishing a direct mechanism by which PI3K promotes MAPK signaling. These two pathways act in parallel and also cooperate with each to stimulate mTOR, which is in turn necessary for both AKT and ERK activations. Last, we show that PI3K, MAPK, and mTOR signaling likely suppresses expression of EGF receptor to promote the budding of the lacrimal gland. Together, these results reveal that the intracellular signaling network can promote budding morphogenesis by controlling cell surface receptor expression.

FGF signaling is the critical inductive signal for lacrimal gland budding. The current model of FGF signaling posits that the adaptor protein Frs2 (Fibroblast Growth Factor Receptor Substrate 2) recruits Grb2 (growth Factor Receptor Bound Protein 2) and Shp2 to activate Ras signaling (*29*). It has also been suggested that Grb2 may interact with Gab1, which binds p85 to activate PI3K signaling (*20*). However, at least in lens development, we have previously shown that *Gab1* is dispensable for FGF signaling (*19*). Here, in the lacrimal gland, we again demonstrated that genetic deletion of *Gab1* did not produce any phenotype. This result is consistent with our previous in vitro data that FGF-induced AKT phosphorylation was unaffected in *Gab1*-deficient cells (*19*). Instead, we confirmed in MEF cells that loss of the Ras-p110α interaction abolished the ability of FGF to activate PI3K signaling (*14*). This interaction is also functionally significant in vivo, as $p110^{RBD}$ mutants displayed reduced pAKT in the lacrimal gland bud and hypoplastic lacrimal gland at birth. These results support the model that FGF-Ras signaling provides the p85-independent route of p110α activation during lacrimal gland development. It is notable that, in both $p110^{RBD}$ and $p110^{CKO}$ mutants, pAKT was down-regulated in the periocular mesenchyme, which correlated with reduction in *Fgf1* expression in the lacrimal gland epithelium. As we have previously demonstrated that deletion of FGF receptors in the neural crest–derived mesenchyme disrupted lacrimal gland budding (*10*), we speculate that the FGF-induced AKT signaling may have been important in both mesenchymal and epithelial compartments during lacrimal gland development.

Although stimulation of PI3K by Ras has been well established, the potential role of PI3K in Ras activation is far less certain (*12*). Nevertheless, a number of studies have presented evidence that PI3K activates MAPK pathway in response to a variety of stimuli, including insulin, integrin, interleukin, G protein–coupled receptor, platelet-derived growth factor, and EGF (*30*–*35*). Here, we showed that FGF-induced MAPK activation was also reduced in $p110^{RBD/RBD}$ MEF cells, demonstrating that PI3K is necessary for FGF-dependent MAPK signaling. Notably, the p110α RBD mutation reduced the ratio of Ras-GTP versus total Ras protein, suggesting that the Ras-p110α interaction may stabilize the active conformation of Ras. In support of the functional role of MAPK downstream to PI3K, we showed that elevation of MAPK signaling activity by expressing $Mek1^{DD}$ could partially ameliorate $p110$ mutant phenotypes. There are likely two reasons for the incomplete rescue in $p110^{CKO}$;$Mek1^{DD}$ mutants. First, since $Mek1^{DD}$ is specific to activating MAPK signaling, it is unlikely to restore other downstream pathways stimulated by PI3K. Second, constitutive expression of $Mek1^{DD}$ could induce the negative feedback mechanism that dampens MAPK activation. Such a scenario has been previously observed in the lacrimal gland, where we showed that oncogenic *Kras* in *Shp2* mutants induced expression of Sprouty2, a negative regulator of MAPK signaling (*9*). Only after deletion of *Sprouty2* could mutant *Kras* fully restore MAPK signaling in *Shp2* mutants. Consistent with this, expression of $Mek1^{DD}$ only resulted in modest up-regulation of pERK in $p110^{CKO}$ mutants. Nevertheless, the attenuation of lacrimal gland phenotype in both $p110^{RBD}$;$Mek1^{DD}$ and $p110^{CKO}$; $Mek1^{DD}$ mutants supports MAPK signaling as a downstream target of PI3K. Together, these results demonstrate that the Ras-p110α interaction serves as an important conduit for PI3K to activate Ras.

mTOR signaling controls cell growth and homeostasis in response to nutrients, energy, and growth factor availability, but its

molecular mechanism in the lacrimal gland has not been studied. We demonstrate that the Raptor-containing mTORC1 complex plays a critical role in lacrimal gland budding. Inactivation of PI3K in lacrimal gland progenitor cells abrogates phosphorylation of mTORC1 downstream targets, S6 and 4EBP1, but not mTOR itself, suggesting that there exists PI3K-independent mechanism(s) of mTOR regulation. Previous in vitro studies have indicated that mTOR inhibitor Tsc2 (Tuberous Sclerosis Complex 2) may be a substrate of Erk and Gsk3 (Glycogen synthase kinase-3), the latter activated by Wnt signaling (25, 26). However, our genetic analysis showed that pmTOR is only dependent on Erk1 and Erk2, not Wnt receptors Lrp5 and Lrp6. These results establish MAPK signaling as a bona fide regulator of mTOR in vivo. We also observed that inhibition of mTOR suppressed ERK phosphorylation both in vitro and in vivo, suggesting that mTOR also regulates MAPK signaling. The cross-regulatory interaction between mTOR and MAPK signaling is supported by genetic rescue experiments, which showed that lacrimal gland development can be induced in mTOR-deficient mutants by expressing $Mek1^{DD}$ to augment MAPK activity. Nevertheless, our attempt to elevate mTOR activity by deleting $Tsc1$ failed to rescue Erk-deficient mutants, showing that mTOR and MAPK signaling also play nonredundant roles during lacrimal gland development.

FGF is the only growth factor thus far implicated in lacrimal gland development, but our study suggests that additional RTK signaling may also play important roles. One inkling is that FGF stimulation can only account for part of PI3K activation in the lacrimal gland bud. Our biochemical and genetic data showed that FGF promotes PI3K signaling via direct binding of Ras to p110α, but disruption of the Ras-p110α interaction only partially reduced PI3K signaling during lacrimal gland development. This is consistent with previous studies indicating that FGF signaling is primarily mediated by Ras-MAPK pathway and, only to a less extent, by PI3K-AKT pathway (36). By transcriptomic analysis, we uncovered the disruption of IGF signaling in $p110$ mutants, but expression of $Igf1$ and $Igf2$ was strongly elevated. This is reminiscent of observations in cancer cells, where inhibition of PI3K signaling frequently leads to increasing expression of upstream RTK ligands and receptors as part of the feedback response. PI3K is the main downstream effector of IGF signaling transmitted by the IGFR-IRS (Insulin Receptor Substrate)-p85 cascade (37), the components of which are highly expressed in the lacrimal gland. It is likely that IGF is the key p85-dependent stimulus for PI3K signaling during lacrimal gland development.

Another dysregulated pathway identified in our study is EGF signaling. Expression of $Egfr$ is normally strong in the bulbar conjunctiva, weak in the palpebral conjunctiva, and absent in the lacrimal gland bud. These distinctions were lost after genetic ablation of $Fgfr2$, $p110$, Erk, or $Raptor$. In $p110^{RBD}$ mutants, Egfr expands from the lacrimal gland stalk into the lacrimal gland bud, which was partly reversed by activation of MAPK signaling in $p110^{RBD}$;$Mek1^{DD}$ mutants. These results suggest that the active FGF-PI3K-MAPK-mTOR signaling in the lacrimal gland bud may be necessary to restrict EGF signaling to the lacrimal gland stalk. Egfr expression could be regulated at the transcriptional level by MAPK-activated transcriptional factors or at the translational level by the PI3K-mTOR axis. The restricted expression of Egfr in lacrimal gland is particularly interesting because the distinction between the stalk and the bud is known to be important for branching morphogenesis. We explored the biological significance of restricted EGF expression using ocular explants, showing that increasing EGF inhibited lacrimal gland budding. It is possible that ectopic EGF signaling disrupts the proximal-distal patterning of the lacrimal gland, which is necessary for specification of the bud. On the other hand, EGF signaling is known to promote proliferation and differentiation of the epidermis (27), which share the developmental origin as the lacrimal gland. EGF signaling may be excluded from the lacrimal gland bud to prevent it from adopting the epidermal fate. Future studies are needed to delineate the mechanism by which EGF signaling plays such a distinctive function. FGF, IGF, and EGF signaling are members of the large RTK signaling family important for development and physiology. Understanding their roles in lacrimal gland development provides a blueprint for future efforts to repair or regenerate lacrimal glands.

METHODS AND MATERIALS
Mice
Mice carrying Le-Cre, $Erk1^{KO}$, $Erk2^{flox}$, $Fgfr2^{flox}$, $Gab1^{flox}$, $p110\alpha^{flox}$, $p110\alpha^{RBD}$ (JAX strain name, $Pik3ca^{tm1Jdo}$/J), $p110\beta^{flox}$, and $Rac1^{flox}$ mice were bred and genotyped as described (17, 19, 38). $p85\alpha^{flox}$ and $p85\beta^{KO}$ were from L. Cantley (Weill Cornell Medicine, New York, NY) (39, 40). $Rictor^{flox}$ and $Raptor^{flox}$ mice were provided by M. A. Rüegg and M. N. Hall (Biozentrum, University of Basel, Basel, Switzerland). $R26R$-LSL-$Mek1^{DD}$ (stock no. 012352) and $Tsc1^{flox}$ (stock no. 005680) mice were originally obtained from the Jackson laboratory and provided by J. Li (University of Connecticut Health Center, Farmington, CT) and S. Tsang (Columbia University, New York, NY), respectively. $Lrp5^{flox}$ (stock no. 026269) and $Lrp6^{flox}$ (stock no. 026267) mouse strains were purchased from the Jackson laboratory. Animals were maintained in a mixed genetic background, and at least three animals were analyzed for each genotype. We did not observe phenotypic difference in lacrimal gland development among Le-cre and $p110\alpha^{flox/flox}$;$p110\beta^{flox/flox}$ mice, and they were used as controls. All animal experiments were performed according to protocols approved by Columbia University Institutional Animal Care and Use Committee.

Laser capture microdissection, RNA-seq, and bioinformatics analysis
Laser capture microdissection and RNA-seq were performed as previously described (21). The RNA-seq data are available at the Gene Expression Omnibus repository under accession number GSE158300. Preprocessing, quality assessment, and differential gene expression analysis of RNA-seq data was carried out in R platform. Differential expression was first tested with the limma R/Bioconductor software package comparing control and experimental groups. The adjusted P values (Adj.P.Val) and fold change (FC) data obtained from limma were visualized in a volcano plot using EnhancedVolcano package. Statistical significance was determined using thresholds of $-\log_{10}(\text{Adj. P. Val}) > 2$ and $|\log_2(\text{FC})| > 1.5$. Unsupervised clustering analysis was performed with the DEseq2 package. Kyoto Encyclopedia of Genes and Genomes pathway enrichment analysis and functional annotation were performed in DAVID. GSEA was performed using a desktop application developed by the Broad Institute. Collection of annotated gene sets were obtained from the Molecular Signatures Database (MSigDB) v7.2 category C5: ontology gene set. Standard (not preranked) GSEA was performed using normalized counts data imported from DESeq2 module. Permutations were set to 1000 for each run, and t test was used to determine statistically significant enrichment. GSEA output data were imported

to R platform to generate enrichment plots following the standard GSEA plot format.

Histology and immunohistochemistry

Histology and immunohistochemistry were performed on the paraffin and cryosections as previously described (*41*, *42*). For pERK, pAKT, p4EBP1, pS6, pmTOR, Sox9, and Sox10 staining, the signal was amplified using a Tyramide Signal Amplification kit (PerkinElmer Life Sciences, Waltham, MA). Antibodies used are Egfr (ab52894) (Abcam); IGF1 (AF791), IGF2 (AF792), IGF1R (AF305), and IGF2R (NB300-514) (Novus Biologicals); FGFR2 (#23328), p4EBP1 (#2855), p85 (#4257), pERK1/2 (#4370), pAKT(#4060), pmTOR (#5536), and pS6 ribosomal protein (#5364) (Cell Signaling Technology); Sox9 (sc-20095) and Sox10 (sc-365692) (Santa Cruz Biotechnology); E-cadherin (#610181) and Ki67 (#550609) (BD Pharmingen); and pHH3 (#06-570) (Millipore). The proliferation rates were calculated as the ratio of pHH-positive cells to 4′,6-diamidino-2-phenylindole–positive cells. The pAKT and pERK fluorescence in lacrimal gland buds were measured by ImageJ and normalized against those in the retina. At least three samples were examined for each genotype. The results were analyzed by *t* test for two samples and one-way analysis of variance (ANOVA) test for three or more samples.

RNA in situ hybridization

Section in situ hybridization was performed as described (*43*). The following probes were used: *Etv4*, *Etv5* (from B. Hogan, Duke University Medical Center, Durham, NC, USA), *Six1* (from B. Morrow, Albert Einstein College of Medicine, New York, NY, USA), *Six2* (from T. Caroll, UT Southwestern Medical center, Dallas, TX, USA), *Dusp6* (IMAGE clone, 3491528) and *Fgf10* (IMAGE clone, 6313081) (from Open Biosystems, Huntsville, AL, USA).

MEF cells and Western blot

Primary MEF cells were isolated from embryos at E13.5 stages and cultured in Dulbecco's modified Eagle's medium (DMEM) containing 10% fetal bovine serum as described (*28*). The cells were starved for 24 to 48 hours before FGF2 (104-02-50, ScienceCell) or IGF1 (291-G1-200, R&D Systems) treatment at 37°C. For gene deletions, MEF cells carrying homozygous flox alleles were infected with Ad5CMV-eGFP or Ad5CMVCre-eGFP (Gene Transfer Vector Core, University of Iowa, IA) in DMEM overnight at a multiplicity of infection of 500 plaque forming units per cell and cultured for 5 days. For inhibitor studies, cells were starved for 24 hours and treated for another 6 hours with PI3K inhibitors LY294002 (50 μM; #9901) and PX866 (1 μM; #13055), MEK inhibitor U0126 (50 μM; #9903), or mTOR inhibitor Torin (150 nM; #14385), all from Cell Signaling Technology. After growth factor stimulation, cells were washed in cold phosphate-buffered saline and harvested in ice-cold CelLytic reagent (C2978, Sigma-Aldrich) supplemented with protease inhibitor cocktail (78841, Thermo Fisher Scientific). Protein samples were denatured at 95°C for 5 min before loaded onto SDS–polyacrylamide gel electrophoresis gels. The antibodies used for Western blot were the same for immunohistochemistry, except anti-pERK1/2 (sc-7383, from Santa Cruz Biotechnology) and anti-ERK1/2 (#4695, Cell Signaling Technology).

Explant culture

Lacrimal gland explant cultures were prepared as previously described (*28*). Briefly, the whole eye, together with the adjacent ectoderm and mesenchyme, was dissected from E13.5 mouse embryos carrying *Le-Cre*. The explants were cultured on a membrane filter (HAWP01300, 0.45-μm pore, Millipore) and covered by Matrigel/DMEM/F12 mixture in the presence or absence of growth factors. Bovine serum albumin (BSA) or EGF (final concentration, 100 ng/ml) were first diluted in DMEM/F12 before mixed with Matrigel in 2:1 ratio. Ten microliter of the mixture was added on top of each explant. In each experiment, one side of embryo was treated with BSA and the other side with EGF. For inhibitor study, IGF inhibitor Picropodophyllin (10 μM; #S7668, Selleckchem), PI3K inhibitor LY294002 (1 mM) and mTOR inhibitor Torin (0.5 μM) were added to the media. After 2 days of incubation at 37°C with 5% CO_2, the explants were examined for GFP-expressing lacrimal gland buds.

REFERENCES AND NOTES

1. S. Wang, R. Sekiguchi, W. P. Daley, K. M. Yamada, Patterned cell and matrix dynamics in branching morphogenesis. *J. Cell Biol.* **216**, 559–570 (2017).
2. D. Zoukhri, Mechanisms involved in injury and repair of the murine lacrimal gland: Role of programmed cell death and mesenchymal stem cells. *Ocul. Surf.* **8**, 60–69 (2010).
3. D. A. Dartt, Neural regulation of lacrimal gland secretory processes: Relevance in dry eye diseases. *Prog. Retin. Eye Res.* **28**, 155–177 (2009).
4. A. Garg, X. Zhang, Lacrimal gland development: From signaling interactions to regenerative medicine. *Dev. Dyn.* **246**, 970–980 (2017).
5. V. Govindarajan, M. Ito, H. P. Makarenkova, R. A. Lang, P. A. Overbeek, Endogenous and ectopic gland induction by FGF-10. *Dev. Biol.* **225**, 188–200 (2000).
6. H. P. Makarenkova, M. Ito, V. Govindarajan, S. C. Faber, L. Sun, G. McMahon, P. A. Overbeek, R. A. Lang, FGF10 is an inducer and Pax6 a competence factor for lacrimal gland development. *Development* **127**, 2563–2572 (2000).
7. Y. Pan, C. Carbe, A. Powers, E. E. Zhang, J. D. Esko, K. Grobe, G. S. Feng, X. Zhang, Bud specific N-sulfation of heparan sulfate regulates Shp2-dependent FGF signaling during lacrimal gland induction. *Development* **135**, 301–310 (2008).
8. A. Garg, A. Hannan, Q. Wang, T. Collins, S. Teng, M. Bansal, J. Zhong, K. Xu, X. Zhang, FGF-induced Pea3 transcription factors program the genetic landscape for cell fate determination. *PLOS Genet.* **14**, e1007660 (2018).
9. Y. Pan, C. Carbe, A. Powers, G. S. Feng, X. Zhang, Sprouty2-modulated Kras signaling rescues Shp2 deficiency during lens and lacrimal gland development. *Development* **137**, 1085–1093 (2010).
10. A. Garg, M. Bansal, N. Gotoh, G. S. Feng, J. Zhong, F. Wang, A. Kariminejad, S. Brooks, X. Zhang, Alx4 relays sequential FGF signaling to induce lacrimal gland morphogenesis. *PLOS Genet.* **13**, e1007047 (2017).
11. J. A. Engelman, J. Luo, L. C. Cantley, The evolution of phosphatidylinositol 3-kinases as regulators of growth and metabolism. *Nat. Rev. Genet.* **7**, 606–619 (2006).
12. M. C. Mendoza, E. E. Er, J. Blenis, The Ras-ERK and PI3K-mTOR pathways: Cross-talk and compensation. *Trends Biochem. Sci.* **36**, 320–328 (2011).
13. P. Rodriguez-Viciana, P. H. Warne, R. Dhand, B. Vanhaesebroeck, I. Gout, M. J. Fry, M. D. Waterfield, J. Downward, Phosphatidylinositol-3-OH kinase as a direct target of Ras. *Nature* **370**, 527–532 (1994).
14. S. Gupta, A. R. Ramjaun, P. Haiko, Y. Wang, P. H. Warne, B. Nicke, E. Nye, G. Stamp, K. Alitalo, J. Downward, Binding of ras to phosphoinositide 3-kinase p110α is required for ras-driven tumorigenesis in mice. *Cell* **129**, 957–968 (2007).
15. E. Castellano, C. Sheridan, M. Z. Thin, E. Nye, B. Spencer-Dene, M. E. Diefenbacher, C. Moore, M. S. Kumar, M. M. Murillo, E. Grönroos, F. Lassailly, G. Stamp, J. Downward, Requirement for interaction of PI3-kinase p110α with RAS in lung tumor maintenance. *Cancer Cell* **24**, 617–630 (2013).
16. M. M. Murillo, S. Rana, B. Spencer-Dene, E. Nye, G. Stamp, J. Downward, Disruption of the interaction of RAS with PI 3-kinase induces regression of EGFR-mutant-driven lung cancer. *Cell Rep.* **25**, 3545–3553.e2 (2018).
17. G. Mathew, A. Hannan, K. Hertzler-Schaefer, F. Wang, G. S. Feng, J. Zhong, J. J. Zhao, J. Downward, X. Zhang, Targeting of Ras-mediated FGF signaling suppresses Pten-deficient skin tumor. *Proc. Natl. Acad. Sci. U.S.A.* **113**, 13156–13161 (2016).

18. Z. Chen, J. Huang, Y. Liu, L. K. Dattilo, S.-H. Huh, D. Ornitz, D. C. Beebe, FGF signaling activates a Sox9-Sox10 pathway for the formation and branching morphogenesis of mouse ocular glands. *Development* **141**, 2691–2701 (2014).

19. H. Li, C. Tao, Z. Cai, K. Hertzler-Schaefer, T. N. Collins, F. Wang, G. S. Feng, N. Gotoh, X. Zhang, Frs2α and Shp2 signal independently of Gab to mediate FGF signaling in lens development. *J. Cell Sci.* **127**, 571–582 (2014).

20. S. H. Ong, Y. R. Hadari, N. Gotoh, G. R. Guy, J. Schlessinger, I. Lax, Stimulation of phosphatidylinositol 3-kinase by fibroblast growth factor receptors is mediated by coordinated recruitment of multiple docking proteins. *Proc. Natl. Acad. Sci. U.S.A.* **98**, 6074–6079 (2001).

21. A. Garg, A. Hannan, Q. Wang, N. Makrides, J. Zhong, H. Li, S. Yoon, Y. Mao, X. Zhang, Etv transcription factors functionally diverge from their upstream FGF signaling in lens development. *eLife* **9**, e51915 (2020).

22. H. Ebi, C. Costa, A. C. Faber, M. Nishtala, H. Kotani, D. Juric, P. Della Pelle, Y. Song, S. Yano, M. Mino-Kenudson, C. H. Benes, J. A. Engelman, PI3K regulates MEK/ERK signaling in breast cancer via the Rac-GEF, P-Rex1. *Proc. Natl. Acad. Sci. U.S.A.* **110**, 21124–21129 (2013).

23. L. Srinivasan, Y. Sasaki, D. P. Calado, B. Zhang, J. H. Paik, R. A. DePinho, J. L. Kutok, J. F. Kearney, K. L. Otipoby, K. Rajewsky, PI3 kinase signals BCR-dependent mature B cell survival. *Cell* **139**, 573–586 (2009).

24. R. Zoncu, A. Efeyan, D. M. Sabatini, mTOR: From growth signal integration to cancer, diabetes and ageing. *Nat. Rev. Mol. Cell Biol.* **12**, 21–35 (2011).

25. K. Inoki, H. Ouyang, T. Zhu, C. Lindvall, Y. Wang, X. Zhang, Q. Yang, C. Bennett, Y. Harada, K. Stankunas, C. Y. Wang, X. He, O. A. MacDougald, M. You, B. O. Williams, K. L. Guan, TSC2 integrates Wnt and energy signals via a coordinated phosphorylation by AMPK and GSK3 to regulate cell growth. *Cell* **126**, 955–968 (2006).

26. L. Ma, Z. Chen, H. Erdjument-Bromage, P. Tempst, P. P. Pandolfi, Phosphorylation and functional inactivation of TSC2 by Erk implications for tuberous sclerosis and cancer pathogenesis. *Cell* **121**, 179–193 (2005).

27. M. Jost, C. Kari, U. Rodeck, The EGF receptor—An essential regulator of multiple epidermal functions. *Eur. J. Dermatol.* **10**, 505–510 (2000).

28. X. Qu, C. Carbe, C. Tao, A. Powers, R. Lawrence, T. H. van Kuppevelt, W. V. Cardoso, K. Grobe, J. D. Esko, X. Zhang, Lacrimal gland development and Fgf10-Fgfr2b signaling are controlled by 2-O- and 6-O-sulfated heparan sulfate. *J. Biol. Chem.* **286**, 14435–14444 (2011).

29. V. P. Eswarakumar, I. Lax, J. Schlessinger, Cellular signaling by fibroblast growth factor receptors. *Cytokine Growth Factor Rev.* **16**, 139–149 (2005).

30. D. A. Cross, D. R. Alessi, J. R. Vandenhede, H. E. McDowell, H. S. Hundal, P. Cohen, The inhibition of glycogen synthase kinase-3 by insulin or insulin-like growth factor 1 in the rat skeletal muscle cell line L6 is blocked by wortmannin, but not by rapamycin: Evidence that wortmannin blocks activation of the mitogen-activated protein kinase pathway in L6 cells between Ras and Raf. *Biochem. J.* **303** (Pt. 1), 21–26 (1994).

31. B. C. Duckworth, L. C. Cantley, Conditional inhibition of the mitogen-activated protein kinase cascade by wortmannin. Dependence on signal strength. *J. Biol. Chem.* **272**, 27665–27670 (1997).

32. B. E. Hawes, L. M. Luttrell, T. van Biesen, R. J. Lefkowitz, Phosphatidylinositol 3-kinase is an early intermediate in the Gβγ-mediated mitogen-activated protein kinase signaling pathway. *J. Biol. Chem.* **271**, 12133–12136 (1996).

33. L. M. Karnitz, L. A. Burns, S. L. Sutor, J. Blenis, R. T. Abraham, Interleukin-2 triggers a novel phosphatidylinositol 3-kinase-dependent MEK activation pathway. *Mol. Cell. Biol.* **15**, 3049–3057 (1995).

34. W. G. King, M. D. Mattaliano, T. O. Chan, P. N. Tsichlis, J. S. Brugge, Phosphatidylinositol 3-kinase is required for integrin-stimulated AKT and Raf-1/mitogen-activated protein kinase pathway activation. *Mol. Cell. Biol.* **17**, 4406–4418 (1997).

35. S. Wennstrom, J. Downward, Role of phosphoinositide 3-kinase in activation of ras and mitogen-activated protein kinase by epidermal growth factor. *Mol. Cell. Biol.* **19**, 4279–4288 (1999).

36. H. Li, Y. Mao, M. Bouaziz, H. Yu, X. Qu, F. Wang, G. S. Feng, C. Shawber, X. Zhang, Lens differentiation is controlled by the balance between PDGF and FGF signaling. *PLOS Biol.* **17**, e3000133 (2019).

37. K. Siddle, Signalling by insulin and IGF receptors: Supporting acts and new players. *J. Mol. Endocrinol.* **47**, R1–R10 (2011).

38. T. N. Collins, Y. Mao, H. Li, M. Bouaziz, A. Hong, G. S. Feng, F. Wang, L. A. Quilliam, L. Chen, T. Park, T. Curran, X. Zhang, Crk proteins transduce FGF signaling to promote lens fiber cell elongation. *eLife* **7**, e32586 (2018).

39. J. Luo, J. R. McMullen, C. L. Sobkiw, L. Zhang, A. L. Dorfman, M. C. Sherwood, M. N. Logsdon, J. W. Horner, R. A. DePinho, S. Izumo, L. C. Cantley, Class IA phosphoinositide 3-kinase regulates heart size and physiological cardiac hypertrophy. *Mol. Cell. Biol.* **25**, 9491–9502 (2005).

40. K. Ueki, C. M. Yballe, S. M. Brachmann, D. Vicent, J. M. Watt, C. R. Kahn, L. C. Cantley, Increased insulin sensitivity in mice lacking p85beta subunit of phosphoinositide 3-kinase. *Proc. Natl. Acad. Sci. U.S.A.* **99**, 419–424 (2002).

41. C. Carbe, K. Hertzler-Schaefer, X. Zhang, The functional role of the Meis/Prep-binding elements in Pax6 locus during pancreas and eye development. *Dev. Biol.* **363**, 320–329 (2012).

42. C. Carbe, X. Zhang, Lens induction requires attenuation of ERK signaling by Nf1. *Hum. Mol. Genet.* **20**, 1315–1323 (2011).

43. C. Carbe, A. Garg, Z. Cai, H. Li, A. Powers, X. Zhang, An allelic series at the paired box gene 6 (Pax6) locus reveals the functional specificity of Pax genes. *J. Biol. Chem.* **288**, 12130–12141 (2013).

Citation: Q. Wang, C. Tao, A. Hannan, S. Yoon, X. Min, J. Peregrin, X. Qu, H. Li, H. Yu, J. Zhao, X. Zhang, Lacrimal gland budding requires PI3K-dependent suppression of EGF signaling. *Sci. Adv.* **7**, eabf1068 (2021).